Pareto Optimal Solutions Visualization Techniques for Multiobjective Design and Upgrade of Instrumentation Networks

Miguel Bagajewicz* and Enmanuel Cabrera

School of Chemical Engineering & Materials Science, University of Oklahoma, 100 E. Boyd Street, T-335, Norman, Oklahoma 73019-1004

Instrumentation networks are essential for the proper operation of chemical plants. This paper addresses the problem of designing and upgrading instrumentation networks. A multiobjective approach is selected to solve the optimization problem, instead of the traditional minimum cost formulation. This paper proposes two methodologies for the visualization of Pareto optimal solutions (POSs) for the design and upgrade of sensor networks: one is based on projections of the POS onto specific two-dimensional surfaces, and the second is the representation of the problem in parallel coordinates systems. The proposed network design algorithms enable the decision maker to see several candidate solutions for the network configuration, and at the same time, they allow the number of candidates to be narrowed to satisfy the decision maker's specifications.

Introduction

Instrumentation is needed in process plants to obtain data that are essential in the performance of several activities: control, quality assurance, production or yield accounting, and fault detection. In addition, the estimation of parameters such as heat exchanger fouling or column efficiencies, among others, is becoming increasingly important, especially for new techniques such as on-line optimization, where the construction of reliable computer models is essential.

The problem of instrumentation network design and upgrade consists of determining the optimal set of instruments such that sufficiently accurate and reliable estimates of variables of interest are obtained, while at the same time bad data due to possible instrument malfunction are filtered.

To solve the cost-optimal design problem, Bagajewicz[1] introduced binary variables to define whether a sensor is measuring a variable. In attempting to define a standard mathematical programming model, he showed that it is not possible to write the constraints explicitly in terms of these binary variables. To sort this difficulty, he used a special branch-and-bound procedure that had some tree-pruning capabilities. Bagajewicz[1] also incorporated a few robustness criteria related to the ability of the network to handle the presence of gross errors (biases, leaks) effectively. Finally, upgrade issues were discussed by Bagajewicz and Sánchez,[2] and the role of maintenance was analyzed by Sánchez and Bagajewicz.[3]

Recently, Chmielewski et al.[4] offered an alternative formulation based on linear matrix inequalities (LMIs) that is convex and can be solved globally. However, integers are still needed in this model. Chmielewski[5] and Chmielewski et al.[6] presented further results of this approach. Finally, Bagajewicz and Cabrera[7] developed an MILP version of the problem based on the idea of assuming that a fake sensor of very large variance and no cost is used for the locations where no sensor is installed, which is the same idea Chmielewski et al.[6] used to construct their model.

One of the difficulties of the present approach[1,4,6,7] is that the model is based on thresholds of different instrumentation network properties (such as residual precision, gross error detectability, resilience, etc.) for which the process engineer has no feeling for the values that should be requested.

To address the aforementioned limitations, a multicriteria approach to the problem has been proposed. In this approach, all of the network features are alternative objectives together with the sensor network cost.[7−10] Viswanath and Narasimhan[10] proposed a general-purpose multiobjective genetic algorithm for sensor network design of linear flow processes. Carnero et al.[9] proposed a procedure based on the application of nondominated sorting genetic algorithms (NSGA) in conjunction with a sharing technique to solve the multiobjective optimal sensor design problem. The advantage of using genetic algorithms is that populations of solutions are processed in every iteration (or generation), whereas classical optimization algorithms use a single solution update in every iteration and a deterministic transition rule between them. Despite the popularity of genetic algorithms, it has been reported that, in linear problems, the performance of genetic algorithms is even worse than that of some classical algorithms.[11]

In this paper, a multiparametric approach based on the MILP formulation proposed by Bagajewicz and Cabrera[7] is used to obtain the Pareto optimal set. Apart from obtaining the Pareto optimal set, it is also important to develop an effective way of visualizing this set so that the decision-making process becomes easier. The main focus of this paper is to propose techniques to visualize these multidimensional Pareto optimal sets. Two ways of visualizing them are proposed: one is based on projections onto two-dimensional surfaces, and the other is based on parallel coordinates representations. A methodology for the decision-making process is also proposed for each type of representation and is illustrated with examples.

* To whom correspondence should be addressed. E-mail: bagajewicz@ou.edu. Tel.: (405) 325-5458. Address: 100 E. Boyd, T-335, Norman, OK, 73019.

Problem Statement

Consider the following optimization problem, which represents one version of the classical cost-minimizing formulation for instrumentation design and upgrade[1]

$$P_1 = \min c_T \quad \text{(cost)}$$

s.t.

$$
\begin{aligned}
\sigma_i \leq \sigma_i^* & \quad \forall \; i \in M_p \quad \text{(precision)} \\
\psi_i \leq \psi_i^* & \quad \forall \; i \in M_p \quad \text{(residual precision)} \\
e_{Di} \leq \kappa_{Di} & \quad \forall \; i \in M_d \quad \text{(error detectability)}
\end{aligned}
\tag{1}
$$

With the exception of precision, the rest of the constraints, together with error resilience, encompass what is known to be a robust network.[1,12] A robust sensor network is one that features meaningful values of precision, residual precision, variable availability, error detectability, and resilience. These five properties encompass the most desired features of a network. In this work, the following criteria were studied:

(a) Residual Precision. Once a redundant measurement is found to have a bias and is eliminated, the overall degree of redundancy is lowered, and the precision of all variables decreases. The *residual precision* of a sensor network is defined as the ability of the network to guarantee a certain level of precision in key selected variables when gross errors are detected and the measurements are eliminated.

(b) Gross Error Detectability. The ability of the network to detect k gross errors of a certain dimensionless size, κ_D or larger, is called error detectability of order k.[1] One can choose a threshold size of gross error for each variable δ_i^* and request that those errors larger than this threshold be detected by the network with a certain statistical confidence level.

(c) Gross Error Resilience. When a gross error of a certain magnitude in any variable occurs and is not detected, a smearing of the corrupted data takes place when reconciliation is performed. The ability of the network to limit the smearing effect of k undetected gross errors of a certain dimensionless size κ_R or lower is called gross error resiliency of order k.[1] The resilience criterion will change when the definition adopted for δ_R is different.[7]

Each one of these robustness criteria can be expressed as linear equations and then be added as constraints to the MILP model. Increasing the levels of the robustness criteria can actually lead to solutions of higher cost or even to infeasibility.[7] Variable reliability and availability constraints can also be added to the problem.[12] In this article, only precision, residual precision, and error detectability are used. The treatment is completely equivalent when more constraints are added to the problem.

It is proposed that problem P_1 be solved as a multiobjective MILP (MOMILP); that is, $P_2 = \min_{\forall i \in M_p, \forall j \in M_d}(c_T, \sigma_i, \psi_i, e_{Dj})$. The goal is to find the set of vectors such that none of their components can be improved without deteriorating at least one of the other components. Such a set of vectors is called a Pareto optimal set (POS).[13]

The POS of the MOMILP problem can be obtained by solving a multiparametric MILP problem (p-MILP)[14]

$$P_3 = \min c_T$$

s.t.

$$
\begin{aligned}
\sigma_i \leq \sigma_i^* & \quad \forall \; i \in M_p, \quad \sigma_{low}^* \leq \sigma_i^* \leq \sigma_{upp}^* \\
\psi_i \leq \psi_i^* & \quad \forall \; i \in M_p, \quad \psi_{low}^* \leq \psi_i^* \leq \psi_{upp}^* \\
e_{Di} \leq \kappa_{Di}^* & \quad \forall \; i \in M_d, \quad \kappa_{low}^* \leq \kappa_i^* \leq \kappa_{upp}^*
\end{aligned}
\tag{2}
$$

This problem is solved for all values of σ_i^*, κ_{Di}^*, and ψ_i^* from lower to upper values. In contrast to many design problems, in this case, it is not difficult to set the values for the bounds of the variables. It is safe to set them from zero to infinity without losing any generality. The algorithm can easily be modified to avoid exploring values for the bounds where there are no feasible solutions.

The solution of this MOMILP problem is a multidimensional POS. Indeed, the number of dimensions of the problem is equal to $d = [1 + 2\text{card}(M_p) + \text{card}(M_d)]$. Because of the dimensions of this problem, it is not straightforward to represent the solutions so that the decision maker can pick good points of the POS. To address this difficulty, iterative methods are usually used.[13] However, instead, we resort to alternative visual representations of the problem and consider two different approaches: two-dimensional projections and parallel coordinates representations.

Two-Dimensional Projections

Consider only cost and precision as the objectives of the problem. Assume also that, instead of minimizing the precision of every stream in M_p, a utility function of all of these precisions is constructed. This function could be the maximum of all precisions, a weighted sum of the precisions, etc. When such an alternative set of objective functions is used, the corresponding POS becomes bidimensional. The same can be done with the residual precision and error detectability. All of these two-dimensional alternative POSs are special points of the Pareto optimal hypersurface.

When error detectability is used as the third objective of the problem, a three-dimensional POS is required. Assume the utility function for error detectability to be equal to the maximum e_{Di} for each i in M_d, that is, $\max(e_{Di}) \; \forall \; i \in M_d$. Likewise, assume that the utility function for precision is $\max(\sigma_i) \; \forall \; i \in M_p$, and the total cost is $c_T = \sum_i \mu_i c_i$, with μ_i being a binary variable stating whether a sensor is located (1) or not (0) in variable i.[1,12] The thresholds for all three objectives are equal to infinity. Thus, the 3D POS is obtained by solving the following problem:

$$P_4 = \min(c_T)$$

s.t.

$$
\begin{aligned}
\max(\sigma) & \leq \sigma^* \\
\max(e_{Di}) & \leq \kappa_D^* \\
\sigma^* & \in [\sigma_{low}^*, \sigma_{upp}^*] \\
\kappa_D^* & \in [\kappa_{low}^*, \kappa_{upp}^*]
\end{aligned}
\tag{3}
$$

Because the problem formulation includes integer variables, we expect the POS to be discrete. The
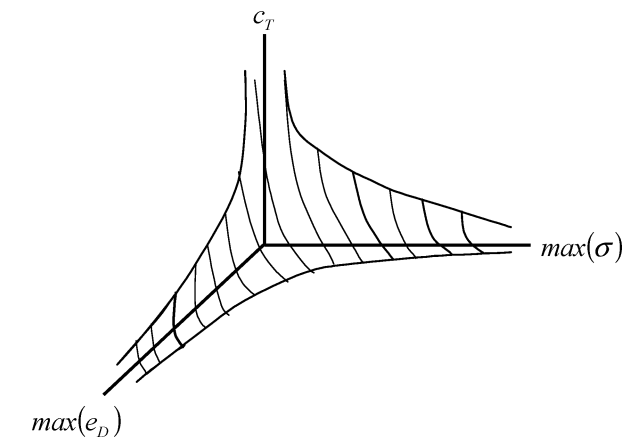
Figure 1. Three-dimensional Pareto optimal set.
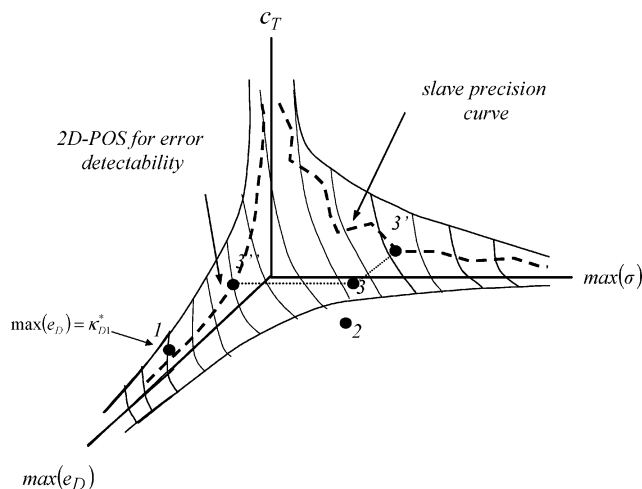

Figure 2. Two-dimensional Pareto optimal sets construction.

schematic surface shown in Figure 1 is the convex hull of such Pareto optimal points for c_T, $\max(\sigma_i)$, and $\max(e_{Di})$.

Fixing one of the threshold parameters, σ_i^* or κ_{Di}^*, and solving problem P_3 again, the solution becomes a 2D POS. For example, if σ_i^* is fixed at its upper value, the following problem is derived:

$$P_5 = \min(c_T)$$

$$\text{s.t.}$$

$$\max(\sigma) = \sigma_{\text{upp}}^*$$

$$\max(e_{Di}) \leq \kappa_D^* \tag{4}$$

$$\kappa_D^* \in [\kappa_{\text{low}}^*, \kappa_{\text{upp}}^*]$$

By solving problem P_5, one obtains the 2D POS for error detectability. The threshold value for precision, σ_i^*, can be fixed at any value between σ_{low}^* and σ_{upp}^*.

We use Figure 2 to illustrate the relationship between 2D and 3D POSs. Assume that problem P_5 is solved for $\kappa_D^* = \kappa_{D1}^*$, with the threshold for precision kept equal to infinity. Assume that the feasible solutions of the problem are the three points highlighted in Figure 2 (points 1–3). Each one represents a different sensor configuration for the system. Points 1 and 3 are feasible points belonging to the Pareto hypersurface, whereas point 2 is a feasible point that is not Pareto optimal. Point 1 lies on the plane $\max(e_{di}) = \kappa_{D1}^*$, but points 2
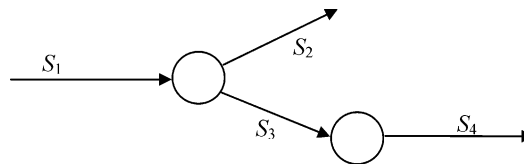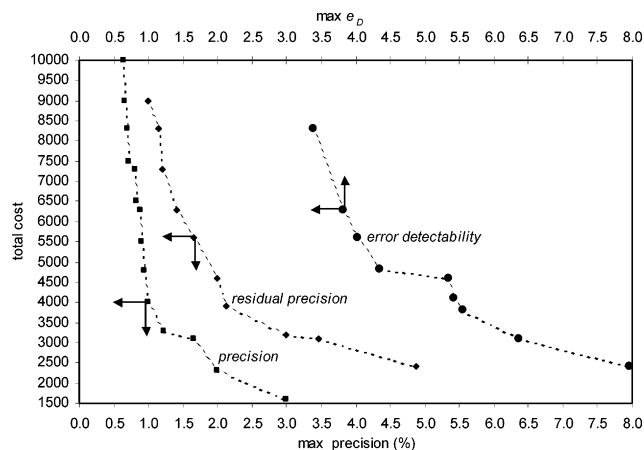

Figure 3. Flowsheet for example 1.

Figure 4. Two-dimensional Pareto optimal sets for example 1.

and 3 do not. Finally, assume that point 3 is the point with the lowest cost among the three. In this situation, point 3 is the optimal solution of the multiparametric problem P_4, and therefore, it is a point of the 2D POS for error detectability (see Figure 2). The whole 2D POS is obtained by solving this same problem for all possible values of κ_D^*.

The projections of all of these special Pareto optimal points onto the c_T vs $\max(e_{Di})$ plane represent the 2D POS for error detectability. The discrete curve created by projecting these same points onto the c_T vs $\max(\sigma_i)$ plane is also a projection of Pareto optimal points. However, because this curve is obtained as a remainder of the process of determining the c_T vs $\max(e_{Di})$ 2D POS, it is called the slave curve. We now illustrate these concepts through an example.

Example 1: Two-Dimensional POS. Consider the process of Figure 3.[1] The flow rates are F (mol/s) = (151.1, 52.3, 97.8, 97.8). Flowmeters with precisions of 3, 2, and 1% are available at costs 800, 1500, and 2500, respectively; M_p is {S_1, S_4}; and M_d includes all measurements.

Two-dimensional POSs based on cost and utility functions for this example are presented in Figure 4. Each point of the graph was obtained by solving MILP problem P_5 using different values for the threshold parameters.

Figure 5 represents the cost vs error detectability POS and the corresponding slave curves for this example. From this type of representation, we can obtain Pareto optimal values of the objectives. For example, for a total cost of 4820 cost units, there is a Pareto optimal configuration with $\max(e_D) = 4.342$, $\max(\sigma) = 1.486$, and $\max(\psi) = 1.486$. Figures 6 and 7 show POS and slave curves for precision and residual precision. Large values in slave curves were omitted.

A procedure for the design of a sensor system is then as follows:

1. The decision maker chooses an objective as the base objective. This does not mean giving this particular objective more importance than the others; it only
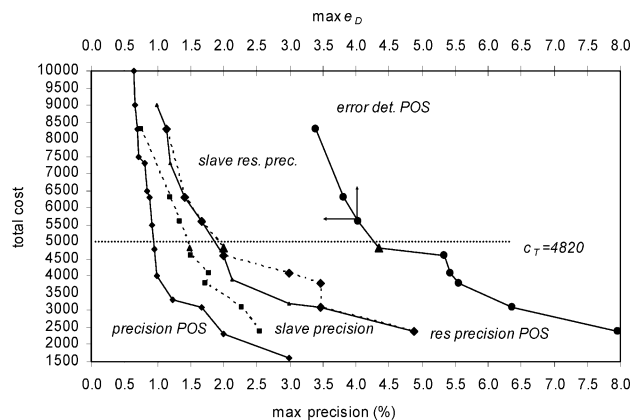
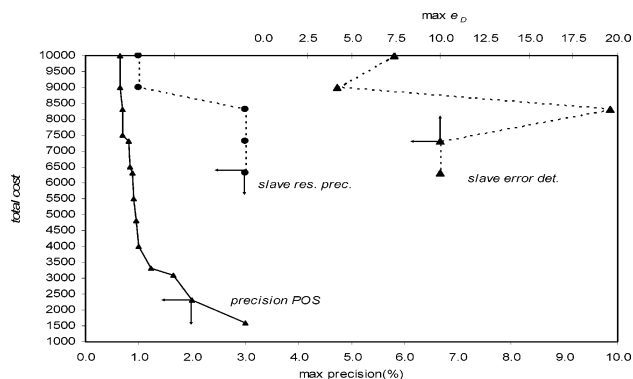**Figure 5.** Cost−error detectability POS and slave curves.

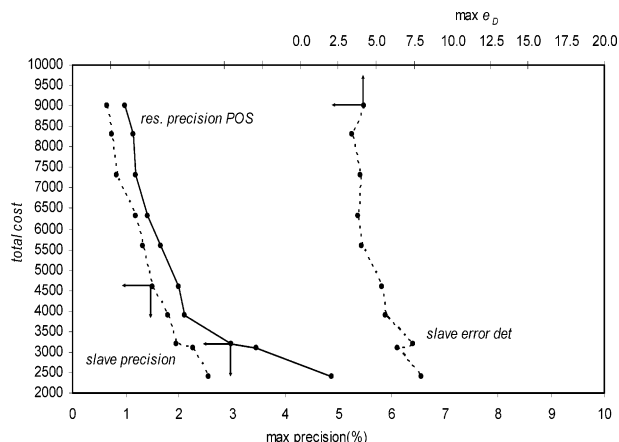**Figure 6.** Cost−precision POS and slave curves.

Figure 7. Cost−residual Precision POS and slave curves.

means that this objective will be the point of reference for the design. Cost seems to be the natural choice.

2. Set maximum allowed values for all objectives. This will set upper bounds for the parameters of the m-parametric problem.

3. Construct all 2D POSs and their slave curves by solving m-parametric problems of the type of P_5. The reference objective will appear in the objective function.

4. Initialize an iteration counter: ite = 1

5. Set the maximum desired value for the base objective. Using this value, obtain candidate solutions from all 2D POSs.

6. If the decision maker is satisfied with at least one of the candidate solutions, then stop. If the decision maker is not satisfied

a. because the reference objective value is too high, then set the maximum desired value of the reference objective lower, or

Table 1. Candidate Solutions for Example 2

from 2D POS for	precision (%)	residual precision (%)	error detectability	cost
precision	0.949	very large	very large	4800
residual precision	1.500	2.0	5.431	4600
error detectability	1.486	2.0	4.342	4800

b. because the values of the other objectives are too high, then set the maximum desired value of reference objective higher.

7. Upgrade the iteration counter: ite = ite + 1

If ite is larger than the maximum allowed number of iterations, then

a. reset the maximum allowed values for all objectives and

b. go to step 2.

8. Go back to step 5.

Example 2. Consider the flowsheet of Figure 3 with all of the specifications of example 1. Assume that the decision maker chooses the total cost as the reference objective for the design. Initially, the values of the other objectives are unrestricted; that is, all upper bounds of the threshold parameters are equal to infinity. With this information, the 2D POSs are constructed. Figure 4 shows these sets.

In this example, the decision maker decides not to spend more than 5000 units of cost on the network. The algorithm found three candidate solutions (Table 1). Notice that the optimal solution from the 2D POS for precision does not provide any residual precision or error detectability capabilities.

Precision is always a very important factor in the design of sensor networks. The candidate solution from the precision 2D POS has a good (low) value for the precision, but it does not provide good results for the other objectives. The question is whether there is a solution with precision between 0.949 and 1.486 that would have some acceptable level of residual precision and error detectability.

Increasing the maximum desired value of the reference objective does not guarantee that candidate solutions with acceptable capabilities for all properties will be obtained. In this situation, it is better to set maximum allowed values for all objectives and reconstruct the slave curves. In terms of the algorithm, upper bounds should be set for all objectives, going back to step 3. In this example, a new 2D POS for precision is constructed, but it now requests the value of κ_D^* to be less than or equal to a certain number, leaving the rest of the objectives unbounded (we pick $\kappa_D^* \leq 8$). Figure 8 presents this discrete set for costs up to 6000.

One can see from Figure 8 that this new POS is above the original one that does not have restrictions for the error detectability upper bound, κ_D^*. Table 2 compares the candidate solutions obtained. This new candidate solution achieves the aforementioned goal of better precision.

Finally, the decision maker chooses one of the three candidate solutions from the 2D POSs. This final decision depends heavily on the particularities of each case, but all three proposed candidates have good network properties. Table 3 presents the location of the sensor in each candidate solution.

Notice that, if the total cost threshold chosen had been less than 3100, the solution from the 2D POS for precision would have been 1.66% for precision and $c_T =$ 3100 (see Figure 4). However, from the same figure,
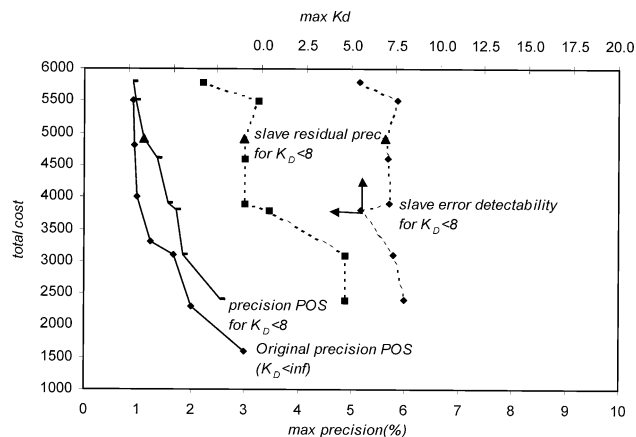
Figure 8. Precision 2D POS for example 2 with $\kappa_d^* \leq 8$.

Table 2. Candidate Solutions from Precision POSs for Example 2

κ_D^*	precision (%)	residual precision (%)	error detectability	cost
<infinite	0.949	very large	very large	4800
≤8	1.126	3.000	6.905	4900

Table 3. Sensor Locations for Candidate Solutions for Example 2

from 2D POS for	sensor locations (%) S_1	S_2	S_3	S_4	c_T	precision (%)	residual precision (%)	e_D
precision	−	2	1	3	4900	1.126	3.000	6.905
residual precision	3	3	3	1	4600	1.500	2.000	5.341
error detectability	1	3	−	2	4820	1.486	2.000	4.342

notice that, by adding only 200 cost units, a much better solution would have been found (1.23% precision). This illustrates the value of visualizing the entire Pareto optimal set, instead of a single solution at a time.

Example 3. Consider the process of Figure 9. Flow-meters of precision 2.5% are available. The cost of the sensor and flow rate for each stream are presented in Table 4. Precision and gross error detection are required for streams S_1, S_2, S_4, S_8, and S_9; that is, $M_p = M_d = \{S_1, S_2, S_4, S_8, S_9\}$.

The total cost of the sensor network is chosen as the reference objective. Upper values for the rest of objectives are set such that all points of the Pareto optimal set provide some level of precision, residual precision, and gross error detectability. In this particular example, only 14 possible configurations from a total of 512 provide precision, residual precision, and error detect-
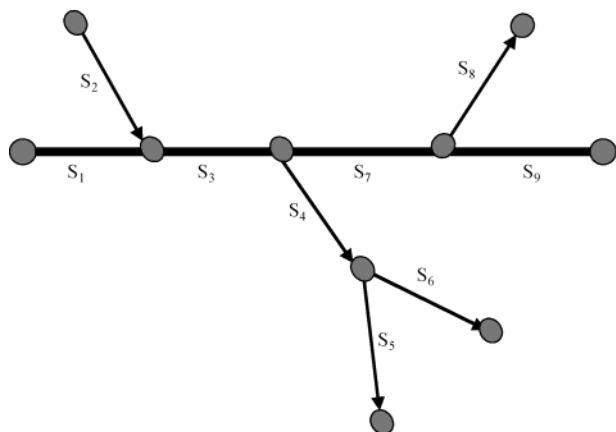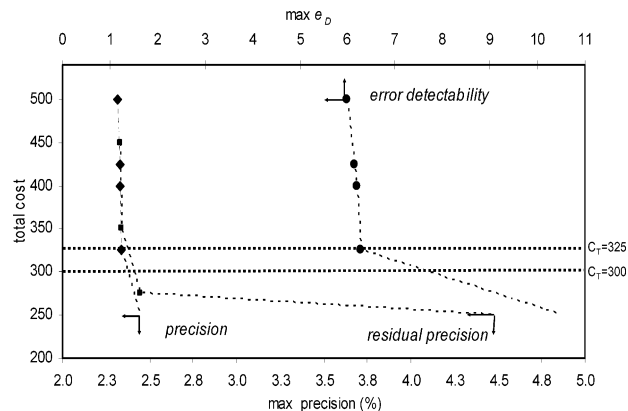

Figure 9. Flowsheet for example 3.

Figure 10. 2D POSs for example 3.

Table 4. Flow Rates and Sensor Costs for Example 3

	flow	sensor cost
S_1	52.30	50
S_2	97.80	75
S_3	150.10	100
S_4	75.05	75
S_5	52.54	50
S_6	22.52	25
S_7	75.05	75
S_8	45.03	30
S_9	30.02	20

Table 5. Candidate Solutions for Example 3 ($c_T < 300$)

from 2D POS for	max precision (%)	max residual precision (%)	error detectability	cost
precision	2.443	4.472	10.502	250
residual precision	2.445	2.443	10.729	275
error detectability	2.443	4.472	10.502	250

Table 6. Candidate Solutions for Example 3 ($c_T < 325$)

from 2D POS for	precision (%)	residual precision (%)	error detectability	cost
precision	2.337	4.323	6.287	325
residual precision	2.445	2.443	10.729	275
error detectability	2.337	4.323	6.287	325

ability capabilities. Figure 10 shows the 2D POSs for this example.

Assuming that the maximum cost to be paid is 300, the candidate solutions in this example are given by the triangle-shaped points in Figure 10, as reported in Table 5.

Notice that the candidate solutions from the precision POS and from the error detectability POS are the same. The values of the error detectability are high for all candidate solutions. Thus, following the proposed procedure, the maximum desired value for the reference objective, total cost, is set higher. Regarding the error detectability set of Figure 10, notice that a much better solution is found with only an additional 25 units of cost. After the maximum cost to pay is set equal to 325, the new candidates obtained are as reported in Table 6.

The candidate solutions from the precision POS and from the error detectability POS are again the same. The final decision in this case depends on which objective, cost or error detectability, is more important for the decision maker. Nevertheless, the solution with lower e_D seems to be better because the increase in the total cost of the network is proportionally smaller than the decrease in e_D. The locations of the sensors for each candidate are presented in Table 7.

Table 7. Sensor Location for Candidate Solutions for Example 3

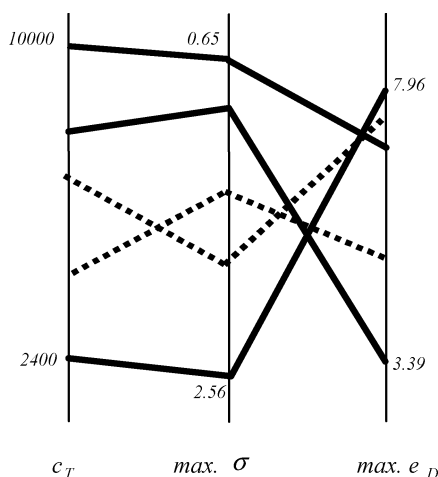| from 2D POS for	c_T	precision (%)	residual precision (%)	e_D	sensor locations
precision	325	2.337	4.323	6.287	$S_1, S_2, S_4, S_7, S_8, S_9$
residual precision	275	2.445	2.443	10.729	$S_1, S_2, S_4, S_6, S_8, S_9$
error detectability	325	2.337	4.323	6.287	$S_1, S_2, S_4, S_7, S_8, S_9$

Figure 11. Parallel coordinates approach.

In summary, by using this approach, the decision maker is able to examine many different optimal solutions at the same time, which provides a better understanding of the problem and, therefore, makes the process of choosing a network easier and more accurate.

Use of Parallel Coordinates

The visualization of multivariate data based on a multidimensional system of parallel coordinates has been studied since 1981 by Alfred Inselberg. His preliminary results on some representations and constructions for N-dimensional lines and hyperplanes appeared in 1981.[15] Interest in this method grew in applications to robotics,[16,17] statistics,[18] and computational geometry,[19] among other areas. Here, we explore its application to sensor network design and upgrade.

The representation consists of placing N copies of the real line, each one representing an objective of the problem (cost, precision, etc.), equidistant and perpendicular to the x axis. These are the axes of the parallel coordinate system for N-dimensional space R^N, all having the same positive orientation as the y axis (although this condition can be conveniently relaxed). A point C with coordinates $(c_1, c_2, ..., c_N)$ is represented by the polygonal line whose N vertexes are at $(i - 1, c_i)$ on the x_i axis for $i = 1, ..., N$.[20]

The key idea is that the description of a higher-dimensional object is captured, to a considerable extent, in the two-dimensional representation of the envelope of the polygonal lines representing its points. Figure 11 presents part of the cost−precision−detectability POS for the flowsheet of Figure 3 in a parallel coordinate system. In this figure, solid lines represent extreme points of the POS, and dotted lines represent intermediate points. Many intermediate points were excluded for simplicity.

For example, Figure 11 shows the cheapest network, $c_T = 2400$, with a maximum precision of $\sigma = 2.56\%$ and an error detectability of $e_D = 7.96$.

This second approach allows all objectives to be observed at the same time, something that is not really possible with the method of 2D POSs. However, when there are many objectives, and therefore many PO points, the problem also becomes harder to visualize in the parallel coordinates system. In addition, this approach does not relate all objectives to the total cost, which can be a drawback when the cost is considered to be the principal objective.

Next is a procedure for the design of sensor network using parallel coordinates systems:

1. Set maximum allowed values for all objectives. This will set upper bounds for the parameters of the m-parametric problem.

2. Obtain the multidimensional PO set by solving the original m-parametric problem P_3. The results are independent of which objective appears in the objective function.

3. Construct the parallel coordinates representation of the PO set. The order of the objectives in the representation does not affect the decision.

4. If the decision maker is satisfied with at least one of the Pareto optimal solutions, then stop. If the decision maker is not satisfied with the solutions or if the data set is too large (and hard to visualize), reset the maximum allowed values for all objectives and go to step 2.

The following examples illustrate the process of obtaining a feasible network configuration using the parallel coordinate system. All of the parallel coordinates representations shown below were obtained using XmdvTool, release 4.0.[21]

Example 4. Consider example 2 with the same characteristics and requirements. The upper bounds are 5% for precision and residual precision and $e_D = 12.0$ for the error detectability, with no upper bound for the cost. There are 69 feasible solutions with these requirements, of which 37 are Pareto optimal.
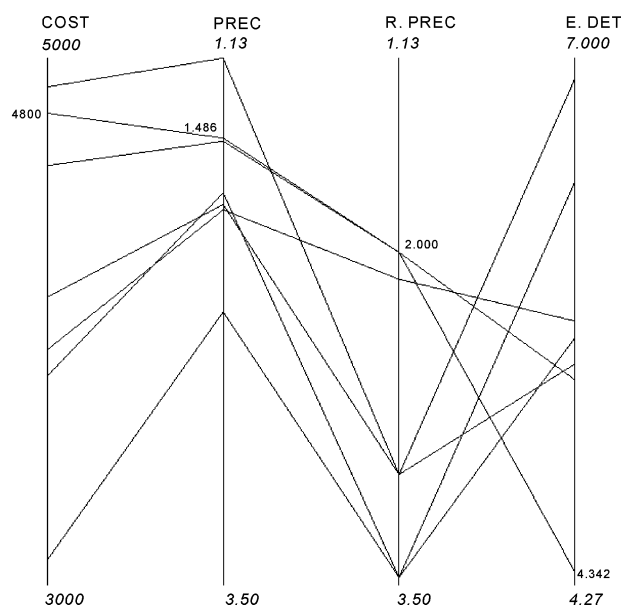
Figure 12 shows the parallel coordinates representation of the PO hypersurface. The scales for precision and residual precision have been inverted to enhance the visualization of the configurations. Notice that, for any given configuration, the precision is always lower than the residual precision. Also, from this figure, it can be seen that, generally, the cheaper the configuration, the worse its characteristics. Nevertheless, this is not always the case.

Notice from the figure that higher costs do not always mean better networks. This is true for all properties studied in this work. In this particular example, the network with the highest cost ($c_T = 10\,000$) presents the best precision and residual precision ($\sigma = 0.648$, $\psi = 1.000$). Nevertheless, the error detectability is not very low for the network with the highest cost ($c_T = 10\,000$), indicating that cost and error detectability are not monotone.

The current data set is too large to clearly differentiate the solutions. The upper bounds are reset to $e_D = 7.00$ for the error detectability and $c_T = 5000$ for the total cost. This generates only seven candidate solutions, making them much easier to differentiate. Figure 13 shows the parallel coordinates representation of the new POS.
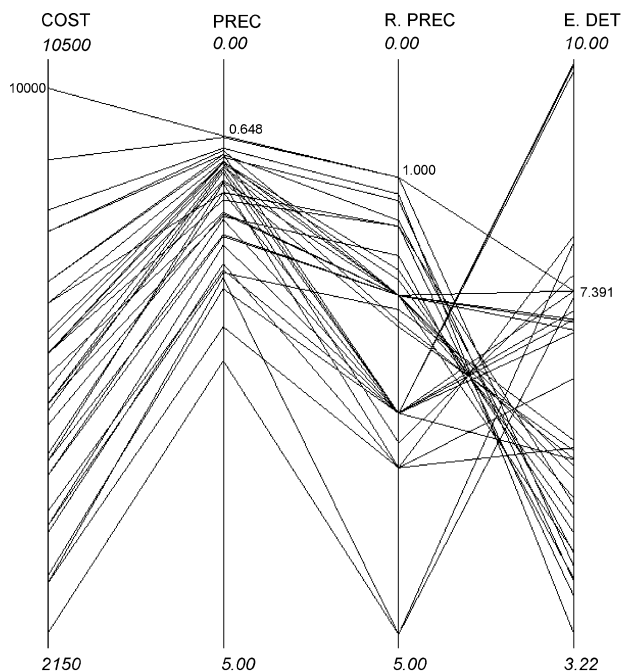
Figure 12. Parallel coordinates representation of POS for example 4 with $e_D \leq 12$.

Figure 13. Parallel coordinates representation of POS for example 4 with $e_D \leq 12.0$.

Table 8. Sensor Locations for the Solution of Example 4

	sensor locations (%)			
solution	S_1	S_2	S_3	S_4
1	1	3	–	2
2	1	3	2	–

Error detectability is probably the most important factor to consider in this situation because the levels of precision, residual precision, and cost are all acceptable. The solution with the lowest e_D value is then chosen. This network has the following features: $c_T = 4800$, $e_D = 4.342$, $\sigma = 1.486\%$, $\psi = 2.000\%$, with two possible sensors location configurations (Table 8).

Example 5. Consider example 3 with the same data and requirements. If we request the network to provide capabilities for all properties, the multidimensional POS

Table 9. Pareto Optimal Set for Example 5

|	c_T	σ (%)	ψ (%)	e_D
1	500	2.320	5.392	5.986
2	450	2.331	2.329	6.175
3	425	2.329	3.603	6.140
4	400	2.332	5.500	6.192
5	350	2.339	2.337	6.310
6	325	2.337	4.323	6.287
7	275	2.445	2.443	10.729
8	250	2.443	4.472	10.502

has only eight points. Table 9 presents these points, and Figure 14 shows its parallel coordinates representation.

For a maximum total cost of 325, there are only three feasible configurations on the POS, the same ones as obtained by using the 2D POS approach. Nevertheless, this second approach provides the decision maker with eight different possible configurations, whereas only two possible solutions were obtained using the first approach.

The network with the cost of 325 has the best features, and thus, it is chosen as the final solution for this problem. One final example illustrating the application of the procedure to retrofit problems is presented next.

Example 6. Consider the network proposed by Madron and Veverka[22] shown in Figure 15. It contains 11 nodes and 24 streams, 9 of which are unmeasured (streams S_1-S_9) and 15 of which are already measured ($S_{10}-S_{24}$). The candidate-stream flow rates to measure are S_1-S_9.

The costs for the sensors added by Meyer et al.[23] and the flow rates considered are presented in Tables 10 and 11, respectively.
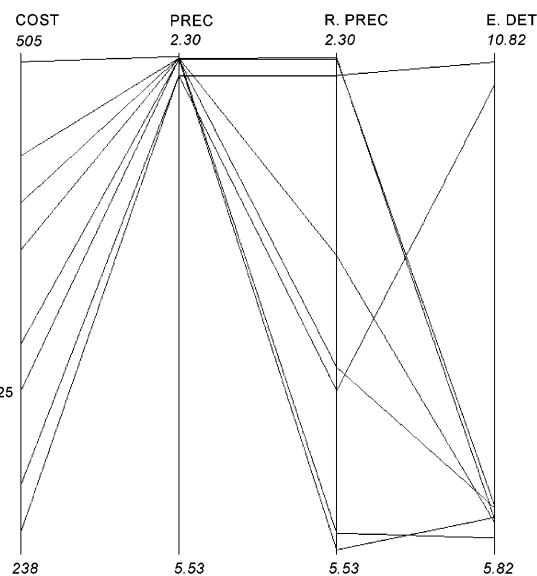
Figure 14. Parallel coordinates representation of POS for example 5.
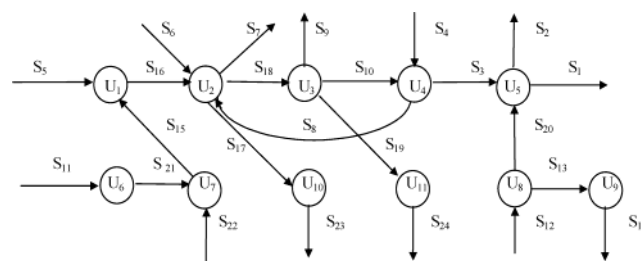
Figure 15. Flowsheet for example 6.[22]

Table 10. Cost of Flowmeters for Example 6[23]

stream	S_1	S_2	S_3	S_4	S_5	S_6	S_7	S_8	S_9
cost	19	17	13	12	25	10	7	6	5

Table 11. Flow Rates Considered for Example 6[23]

stream	flow	stream	flow	stream	flow
S_1	140	S_9	10	S_{17}	5
S_2	20	S_{10}	100	S_{18}	135
S_3	130	S_{11}	80	S_{19}	45
S_4	40	S_{12}	40	S_{20}	30
S_5	10	S_{13}	10	S_{21}	80
S_6	45	S_{14}	10	S_{22}	10
S_7	15	S_{15}	90	S_{23}	5
S_8	10	S_{16}	100	S_{24}	45

Assume that all of the candidate and existing sensors have a precision of 2.5%. Precision and residual precision are required for streams S_1-S_5, whereas gross error detection is required for streams S_1 and S_3, which have the largest flow rates. Thus, $M_p = \{S_1, S_2, S_3, S_4, S_5\}$ and $M_d = \{S_1, S_3\}$.

If the network is requested to provide capabilities for all properties, the POS has 20 points. This example studies both proposed visualization approaches.

a. Parallel Coordinates. The parallel coordinates representation of the POS is presented in Figure 16.

Notice that, for a relatively small range of costs, the obtained candidate solutions show very different levels of precision and residual precision. However, the error detectability falls in a small range of values. Following the proposed algorithm, the maximum values for the precision and residual precision are set to be less than 5%, that is, σ, $\psi \leq 5\%$. The parallel coordinates representation of the new PO set is presented in Figure 17.

The number of candidate solutions is reduced to 14. The level in every property is acceptable for all candidate networks. Because all candidate solutions are acceptable, a new criterion is needed to select the final solution. This means that the decision maker has to take one or some of the objectives as more important than the rest to differentiate the networks.

Assuming, for the example, that the decision maker wants to rank the solutions according to the error detection capabilities of the network, the configuration
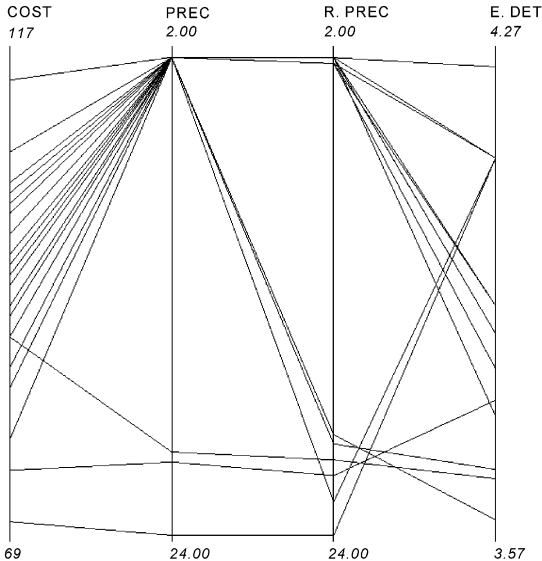

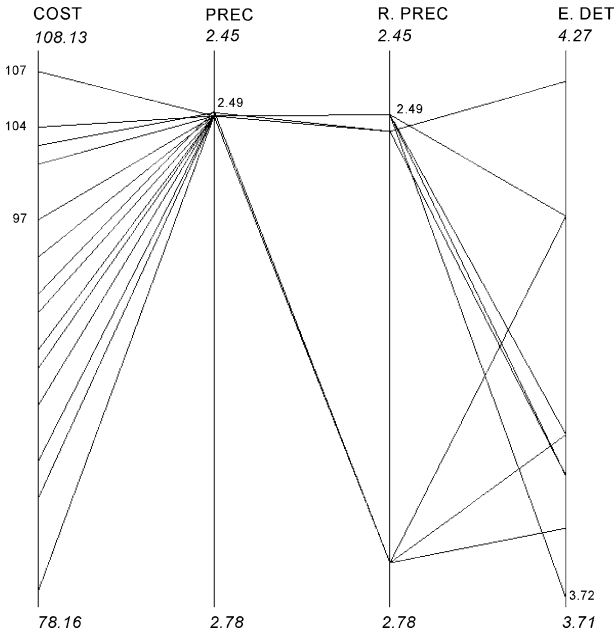**Figure 16.** Parallel coordinates representation of POS for example 6.

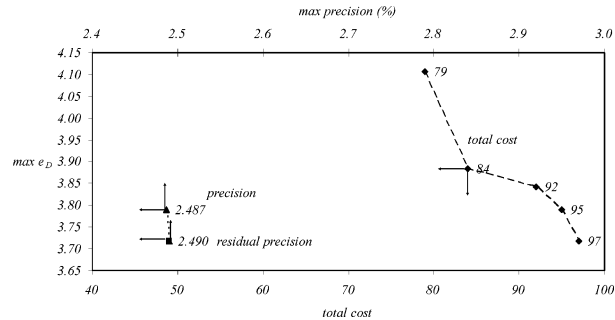**Figure 17.** Parallel coordinates representation of POS for example 6 with σ, $\psi \leq 5\%$.

Figure 18. 2D POSs for example 6.

Table 12. Advantages and Disadvantages of the Two Methods

2D POS	Parallel Coordinates
generally easier to visualize	more candidate solutions are available
all 2D POS must be examined to get a satisfactory sensor network	just one graph is necessary to obtain a network
does not allow all objectives to be seen at the same time.	all objectives can be seen at the same time
labor-intensive when there are many objectives	visualization is harder when there are many objectives

chosen is the one with the lowest value for $\max(e_D)$ (see Figure 17). There are three different configurations with the same value for $\max(e_D)$ (see Figure 17); of these three, the network with the lowest cost was chosen. This network has sensors located in all streams excepting S_6 and S_8, $\max(e_D) = 3.718$, $c_T = 97$, and $\max(\sigma) = \max(\psi) = 2.490\%$.

b. Two-Dimensional Projections. The reference objective is error detectability. The maximum values for the precision and residual precision are set to be less than 5%, that is, σ, $\psi \leq 5\%$. Figure 18 shows the two-dimensional POSs for this example.

Because all candidate solutions are acceptable, the configurations with lower values for $\max(e_D)$ are selected from each 2D POS. The same configuration is obtained from all three sets, with sensors located in all streams except S_6 and S_8, $\max(e_D) = 3.718$, $c_T = 97$, and $\max(\sigma)$

$= \max(\psi) = 2.490\%$. This is the same solution obtained with the parallel coordinates approach.

Table 12 provides a comparison of the advantages and disadvantages of the two methods.

Conclusions

This work proposes two POS visualization techniques for multiobjective design and upgrade of sensor networks. The first methodology is based on projections of the Pareto optimal set onto specific two-dimensional surfaces, and the second is the representation of the problem in parallel coordinates systems. Both approaches were studied and compared. The use of parallel coordinates proved to be more effective for the cases were the POS is not very large, whereas the two-dimensional representations are easier to visualize but require more computation time. The main contribution is the construction of efficient algorithms for the design of sensor networks. These design algorithms are quite valuable because they can accelerate the decision-making process and make it more meaningful. It was shown that the use of these algorithms enables the decision maker to see several candidate solutions for the network configuration and narrow down the number of candidates to satisfy the decision maker's specifications.

Acknowledgment

Nomenclature

c_i = cost of sensor for stream i
c_T = total cost of the network
e_{Di} = dimensionless gross error of variable i
F_i = flow rate of stream i
M = set of all variables
M_d = subset of M for which error detectability is required
M_p = subset of M for which precision or residual precision is required
$\hat{s}$ = variance of estimates from data reconciliation
s_i^* = threshold for the variance of variable i
S_i = stream i

Greek Letters

μ_i = binary variable stating whether a sensor is located (1) or not (0) in variable i
ψ_i^* = threshold for the residual precision of variable i
ψ_i = residual precision of variable i
ψ_{low}^*, ψ_{upp}^* = lower and upper bounds, respectively, for ψ_i^*
κ_{low}^*, κ_{upp}^* = lower and upper bounds, respectively, for κ_D^*
σ_{low}^*, σ_{upp}^* = lower and upper bounds, respectively, for $\hat{s}_i$
κ_D^* = dimensionless threshold value for the error detectability

Literature Cited

(1) Bagajewicz, M. Optimal Sensor Location in Process Plants. *AIChE J.* **1997**, *43*, 9, 2300.

(2) Bagajewicz, M.; Sanchez, M. Reallocation and Upgrade of Instrumentation in Process Plants. *Comput. Chem. Eng.* **2000**, *24*, 8, 1961−1980.

(3) Sánchez, M.; Bagajewicz, M. On the Impact of Corrective Maintenance in the Design of Sensor Networks. *Ind. Eng. Chem. Res.* **2000**, *39*, 4, 977−981.

(4) Chmielewski, D.; Palmer, T. E.; Manousiouthakis, V. Cost Optimal Retrofit of Sensor Networks with Loss Estimation Accuracy. Presented at the AIChE Annual Meeting, Dallas, TX, Oct 31−Nov 5, 1999.

(5) Chmielewski, D. Convex Methods in Sensor Placement. In *Proceedings of the 4th IFAC Workshop on On-Line Fault Detection & Supervision in the Chemical Process Industries*; Elsevier Science: New York, 2001.

(6) Chmielewski, D.; Palmer, T. E.; Manousiouthakis, V. On the Theory of Optimal Sensor Placement. *AIChE J.* **2002**, *48*, 5, 1001−1012.

(7) Bagajewicz, M.; Cabrera, E. A New MILP Formulation for Instrumentation Network Design and Upgrade. *AIChE J.* **2002**, *48*, 10, 2271−2282.

(8) Carnero, M.; Hernandez, J.; Sanchez, M. C.; Bandoni, A. An Evolutionary Approach for the Design of Nonredundant Sensor Networks. *Ind. Eng. Chem. Res.* **2001**, *40*, 5578−5584.

(9) Carnero, M.; Hernandez, J.; Sanchez, M. C.; Bandoni, A. Multiobjective Evolutionary Optimization in Sensor Network Design. In *Proceedings of ENPROMER 2001*; 2001; Vol. I, pp 325−330.

(10) Viswanath, A.; Narasimhan, S. Multiobjective Sensor Network Design Using Genetic Algorithms. In *Proceedings of the 4th IFAC Workshop on On-Line Fault Detection & Supervision in the Chemical Process Industries*; Elsevier Science: New York, 2001.

(11) Deb, K. *Multiobjective Optimization Using Evolutionary Algorithms*; John Wiley & Sons Ltd. :Chichester, U.K., 2001.

(12) Bagajewicz, M. *Design and Upgrade of Process Plant Instrumentation*; Technomic: Lancaster, PA,2000.

(13) Miettinen, K. *Nonlinear Multiobjective Optimization*; Kluwer Academic Publishers: Boston, 1999.

(14) Papalexandri, K.; Dimkou, T. A Parametric Mixed-Integer Optimization Algorithm for Multiobjective Engineering Problems Involving Discrete Decisions. *Ind. Eng. Chem. Res.* **1998**, *37*, 1866−1882.

(15) Inselberg, A. *N-Dimensional Graphics Part I: Lines and Hyperplanes*; IBM LA Science Center Report No. G320-2711; IBM Corporation: White Plains, NY, 1981.

(16) Cohan, S. M.; Yang, D. C. H. Mobility analysis of planar four-bar mechanisms through the parallel coordinate system. *J. Mech. Mach. Theory* **1986**, *21*, 63−67.

(17) Fiorini, P.; Inselberg, A. Configuration Space Representation in Parallel Coordinates. In *Proceedings of the IEEE Conference on Robotics and Automation*; IEEE Press: Piscataway, NJ, 1989; pp 1215−1219.

(18) Wegman, E. Hyperdimensional Data Analysis Using Parallel Coordinates. *J. Am. Stat. Assoc.* **1990**, *411* (85), 664−665.

(19) Inselberg, A.; Reif, M.; Chomut, T. Convexity Algorithms in Parallel Coordinates. *J. ACM* **1987**, *34*, 765−801.

(20) Inselberg, A.; Dimsdale, B. Parallel Coordinates−A Tool for Visualizing Multivariate Relations. In *Human−Machine Interactive Systems*; Klinger, A., Ed.; Plenum Publishing Corporation: New York, 1991.

(21) Ward, M.; Allen, R. M.; Ying-Huey, F.; Jim Y. *The Multivariate Data Visualization Tool*; Worcester Polytechnic Institute: Worcester, MA, 1994−1999; http://davis.wpi.edu/~xmdv/ (accessed May 2002).

(22) Madron, F. *Process Plant Performance. Measurement and Data Processing for Optimization and Retrofits*; Ellis Horwood: West Sussex, U.K., 1992.

(23) Meyer, M. J.; Le Lann, L.; Koehret, B.; Enjalbert, M. Optimal Selection of Sensor Location on a Complex Plant Using a Graph Oriented Approach. *Comput. Chem. Eng.* **1994**, *18*, S535−S540.